Available online at www.sciencedirect.com
ScienceDirect
Journal of Magnetic Resonance 190 (2008) 171–182
JMR Journal of Magnetic Resonance
www.elsevier.com/locate/jmr

^{1}H-Detected IPAP DEPT-INADEQUATE and IPAP RINEPT-INADEQUATE for the measurement of long-range carbon–carbon coupling constants

Lan Jin [a], Katalin E. Kövér [b], Marc R. Lenoir [a], Dušan Uhrín [a,*]

[a] School of Chemistry, University of Edinburgh, West Mains Road, Edinburgh EH9 3JJ, UK
[b] Department of Inorganic and Analytical Chemistry, University of Debrecen, Egyetem tér 1, H-4010 Debrecen, Hungary

Received 22 June 2007; revised 27 September 2007
Available online 1 November 2007

Abstract

The sensitivity of cryoprobes, which are rapidly becoming available, have brought about the possibility of measurement of ^{13}C, ^{13}C coupling constants at the natural abundance of ^{13}C using tens rather than hundreds of milligrams of compounds. This relatively recent development lays the foundation for a more routine use of the ^{13}C, ^{13}C long-range coupling constants in the conformational analysis of molecules. We have designed novel ^{1}H-detected INADEQUATE experiments optimized for long-range ^{13}C, ^{13}C correlations and the measurement of long-range coupling constants. These experiments incorporate refocusing of $^{1}J_{CH}$ coupling constants prior to the formation of DQ coherences and ^{1}H-decoupling during the long carbon–carbon evolution intervals. Such modifications significantly enhance their performance over ^{1}H-detected INADEQUATE experiments currently in use for mapping the one-bond ^{13}C, ^{13}C correlations. ^{1}H or ^{13}C polarization is used a starting point in long-range correlation ^{1}H-detected IPAP DEPT-INADEQUATE or RINEPT-INADEQUATE experiments. These correlation experiments were modified yielding in-phase (IP) or antiphase (AP) ^{13}C, ^{13}C doublets in F_1. Procedures were developed for their editing yielding accurate values of small ^{13}C, ^{13}C coupling constants. The methods are illustrated using mono- and disaccharide samples and compared with related ^{13}C-detected experiments by means of the measurement of interglycosidic ^{13}C, ^{13}C coupling constants of a disaccharide.

Keywords: NMR spectroscopy; INADEQUATE; IPAP; Long-range carbon–carbon coupling constants; Conformational analysis; Carbohydrates

1. Introduction

Long-range carbon–carbon coupling constants, $^{n}J_{CC}$, report on the stereochemistry and conformation of molecules [1–6] in a similar manner as the more easily accessible proton–proton or proton–carbon long-range coupling constants. Low sensitivity of NMR experiments performed at the natural abundance of ^{13}C has thus far hindered a more wide spread utilization of $^{n}J_{CC}$ couplings in the conformational analysis of small and medium size molecules. However, a recent introduction of cryogenic probes has reduced sample requirements dramatically. In principle, tens rather than hundreds of milligrams of medium size molecules are now sufficient for the measurement of $^{n}J_{CC}$ coupling constants.

Practically all NMR experiments designed to select carbon pairs in natural abundance ^{13}C molecules use ^{13}C–^{13}C DQ filtration—the principle introduced for the first time in the seminal INADEQUATE experiments [7,8]. Since then, numerous variations of the INADEQUATE have appeared in the literature. The early experiments focusing on the measurement of $^{n}J_{CC}$ coupling constants were performed using ^{13}C-detection [9–13]; more recently, several ^{1}H-detected methods have been proposed [14–17]. The existing methods can be classified as intensity based [15], *J*-resolved [9,14] and *J*-modulated correlation [10–13,16,17] techniques. The latter two types achieve the

* Corresponding author. Fax: +44 131 650 7155.
E-mail address: dusan.uhrin@ed.ac.uk (D. Uhrín).

1090-7807/$ - see front matter © 2007 Elsevier Inc. All rights reserved.
doi:10.1016/j.jmr.2007.10.016

determination of coupling constants in the frequency [9–14,16] or the time domain [17]. Due to the nature of the INADEQUATE, cross peaks in the ^{13}C-detected experiments appear in F_2 as antiphase doublets with regard to J_{CC} coupling. Similarly, *J*-resolved [9,14] or *J*-modulated techniques produce antiphase doublets [16,18] or multiplets [17] in F_1. This is not a problem when dealing with large $^1J_{CC}$ coupling constants. However, the determination of small $^nJ_{CC}$ coupling constants is not trivial, as partial cancellation of closely spaced antiphase lines produces an apparent splitting that is larger than the true coupling constant [19,20]. A *J*-modulated ADEQUATE experiment [16], which presents in-phase doublets in F_1, leads to a more accurate determination of $^nJ_{CC}$ coupling constants when using peak picking procedures. Nevertheless, also this method fails for unresolved doublets. Analyzing antiphase doublets using line fitting, as a way of determining the coupling constants, is problematic even if the line widths are known through the measurement of relaxation times. This is due to the fact that different combinations of *J* couplings and peak heights can reproduce the experimental doublets equally well, which is particularly true for poorly resolved doublets and noisy INADEQUATE spectra.

It has been illustrated by numerous NMR experiments that editing of the corresponding in- and antiphase multiplets is a possible route towards accurate determination of coupling constants from unresolved multiplets [20–24]. This approach has since been successfully applied under the acronym IPAP [25] to the measurement of scalar and residual dipolar coupling constants of biomolecules. We have recently used this principle to design a ^{13}C-detected IPAP-INADEQUATE experiment and demonstrated its efficiency in accurate measurement of small $^nJ_{CC}$ coupling constants [13]. In this work, we apply the same principle to ^{1}H-detected INADEQUATE experiments. Two ^{1}H-detected IPAP-INADEQUATE experiments are introduced with the aim to maximize the sensitivity and accuracy of the measurement of $^nJ_{CC}$ coupling constants.

2. Materials and methods

The samples used throughout this work were prepared by dissolving 70 mg of Me-β-D−xylopyranoside (**I**, $M_W = 164.2$ g/mol) and 25 mg of Me-β-D-lactoside (**II**, $M_W = 356$ g/mol) (Fig. 1) in 350 μL of D_2O and transferred to Shigemi tubes. All ^{1}H-detected INADEQUATE spectra of **I** and **II** were acquired using a 600 MHz triple-resonance cryoprobe with *z*-gradients. The T_2 and T_2^* relaxation times of **I** and **II** were determined, respectively, by acquiring a series of ^{13}C spin-echoes (effectively 90-Δ_2-180-Δ_2 of the INADEQUATE pulse sequence) with and without the ^{1}H decoupling and using maximum evolution times $>2T_2$. The ^{13}C T_1 relaxation times were determined using the inversion recovery method with ^{1}H decoupling during the recovery delay. The T_1 relaxation times of ^{13}C-attached protons were determined using the inversion recovery sequence followed by a gradient selected 1D HSQC. The peak intensities were fitted as single exponential decays to determine the decay constants.

The three long-range carbon–carbon correlation spectra of **I** were acquired using the pulse sequences of Fig. 1 and the t_1 and t_2 acquisition times of 23 and 102 ms, respectively. The relaxation time was set to 1.3 s, 16 scans were acquired in each of 192 complex points. Delays τ, and τ_2 were optimized for $^1J_{CH} = 150$ Hz as 1/2 $^1J_{CH}$ 1/4 $^1J_{CH}$, respectively; τ_1 in the RINEPT was optimized for all multiplicities (2.0 ms) and Δ_2 was set to $1/4^nJ_{CC}$ ($^nJ_{CC} = 3.0$ Hz) for all experiments. θ was set to 90° in the DEPT-based pulse sequence. The overall experimental time was 3.2 h for each individual experiment. The 90° BEBOP and 180° BIBOP pulses [40,41] were 700 and 1400 μs long and applied at $\gamma B_1/2\pi = 12.5$ kHz. A 500 μs adiabatic pulse ^{13}C pulse was used to invert the carbon z magnetization.

The IPAP DEPT-INADEQUATE and IPAP RINEPT-INADEQUATE spectra of **II** (Fig. 2) were acquired using the pulse sequences of Fig. 3a–d, respectively. Relaxation times of 1 and 1.3 s were used, respectively. This corresponds to 2.3 times of the longest T_1 relaxation time of ^{13}C and ^{1}H attached to ^{13}C, respectively. The in- and antiphase spectra were acquired in an interleaved mode using 24 scans in each of 875 complex points. The t_1, κt_1 and t_2 acquisition times of 102, 408 and 103 ms, respectively were used. Scaling factor, $\kappa = 4$ was applied during the *J*-evolution. The evolution interval, $2\Delta_2$, was optimized for $^nJ_{CC} = 3.0$ Hz ($\Delta_2 = 1/4^nJ_{CC}$). A 20 ms adiabatic pulse [42] was applied simultaneously with low level PFGs. The total experimental time was 47.5 and 41.5 h for the IPAP DEPT-INADEQUATE and IPAP RINEPT-INADEQUATE experiments, respectively. The 2D spectra were zero filled to yield a digital resolution of 0.25 Hz/point in F_1. No window function was used in F_1. ^{13}C-detected IPAP INADEQUATE spectra of **II** were acquired using an 800 MHz triple-resonance cryoprobe with *z*-gradients and a cold carbon preamplifier as detailed in [13].

3. Results

3.1. Long-range carbon–carbon correlation

The relaxation of coherences affects the sensitivity of NMR experiments and additionally, in *J*-resolved/*J*-modulated experiments, the line widths of spectral lines. The coherences that evolve during the long-range evolution intervals of ^{1}H-detected INADEQUATE [26] (Fig. 1a) can be written as $\prod_{n=0}^{k} H_{n,z} C_{1,xy}$ and $\prod_{n=0}^{k} H_{n,z} C_{1,xy} C_{2,z}$, where k is the number of protons coupled to C_1 via one-bond or long-range couplings and C_1 and C_2 are the two coupled carbons. Both ^{13}C transverse and ^{1}H and ^{13}C longitudinal relaxation (spin-flips) contribute to the decay of these coherences. During the DQ frequency labelling period, the following coherences exist: $\prod_{n=0}^{k} H_{n,z} C_{1,xy}$

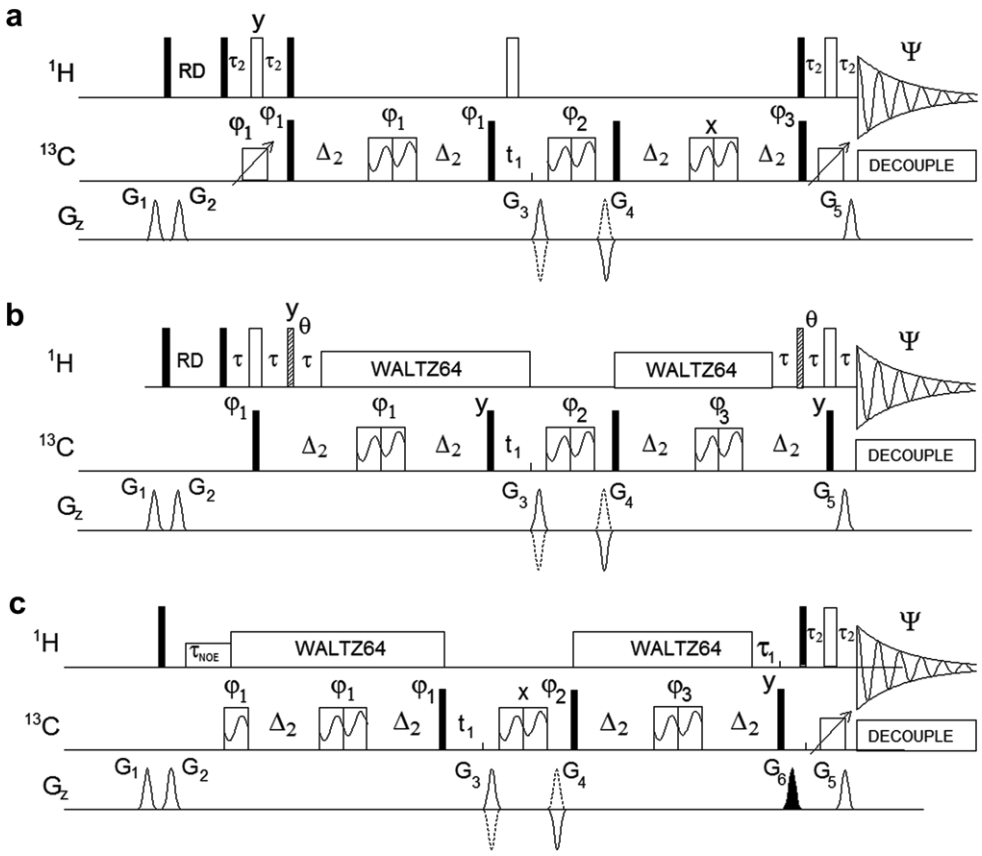

Fig. 1. Pulse sequences of ^{1}H-detected INEPT-INADEQUATE (a), DEPT-INADEQUATE (b) and RINEPT-INADEQUATE (c). The filled and open rectangles represent 90° and 180° rectangular pulses, respectively, applied from the x axis unless stated otherwise. The dashed rectangles of the DEPT pulse sequence represent rectangular pulses with flip angle $\theta = 90°$ or 45°. The 90° BEBOP [40] and 180° BIBOP pulses [41] are indicated as wide rectangles with a sine wave. The adiabatic inversion pulse is identified by an inclined arrow. The following delays were used: $\tau = 0.5/^1J_{CH}$, $\Delta_2 = 0.25/^nJ_{CC}$, $\tau_1 = 0.5/^1J_{CH}$ for CH and $0.3/^1J_{CH}$ for all multiplicities, $\tau_2 = 0.25/^1J_{CH}$, RD is relaxation delay. All PFGs were shaped according to a CHIRP pulse [42] and applied during 1 ms, with an exception of G_6 that was applied for 2 ms. The echo-antiecho encoding of F_1 frequencies was achieved by changing the sign of G_3 and G_4 PFGs between successive t_1 increments. PFGs expressed as a percentage of 50 Gcm^{-1} were: $G_1 = 57\%$, $G_2 = 77\%$, $G_3 = 40\%$, $G_4 = -40\%$, $G_5 = 40.16\%$, $G_5 = 90\%$. The following phase cycling was applied in (a): $\varphi_1 = x, y, -x, -y$; $\varphi_2 = x, y, -x, -y, -x, -y, x, y$; $\varphi_3 = 8x, 8(-x)$; $\Psi = 4(x, -x), 4(-x, x)$. The following phase cycling was applied in (b): $\varphi_1 = x, -x$; $\varphi_2 = 2x, 2(-x)$; $\varphi_3 = 8x, 8y$; $\Psi = 2(x, -x), 2(-x, x)$. The following phase cycling was applied in (c): $\varphi_1 = x, y, -x, -y$; $\varphi_2 = 4x, 4(-x)$; $\varphi_3 = 8x, 8(y)$; $\Psi = 2(x, -x), 4(-x, x), 2(x, -x)$.

$C_{2,xy}\prod_{m=0}^{l}H_{m,z}$, where k and l is the number of C_1 and C_2 coupled protons. It has been demonstrated before [27,28] that removing the proton terms from heteronuclear coherences prolongs their lifetime. In the context of the ^{1}H-detected INADEQUATE this can be achieved by refocusing the one-bond proton–carbon couplings and applying ^{1}H decoupling during most of the pulse sequence. Under these circumstances the relevant coherences present during the evolution and DQ labelling intervals simplify to $C_{1,xy}$, $C_{1,xy}C_{2,z}$ and $C_{1,xy}C_{2,xy}$. Although this modification is not required for $^1J_{CC}$ optimized experiments, it becomes important for long-range correlation experiments containing long evolution intervals. In practise, as the carbon magnetization needs to be defocused with regard to the one-bond couplings prior to its back transfer to protons for detection, this approach results in modified INADEQUATE pulse sequences containing one refocusing and one defocusing delay. The optimal setting of these intervals can only be achieved for CH groups. Starting the experiment with ^{13}C magnetization and using the reverse INEPT (RINEPT) pathway [29] eliminates the need for the first refocusing interval and results in a more efficient optimization of the experiments for all carbon multiplicities.

Before proceeding with the implementation of these ideas, we will inspect the relaxation properties of relevant coherences using two model compounds, of Me-β-D−xylopyranoside (**I**, $M_W = 164.2$ g/mol) and Me-β-D-lactoside (**II**, $M_W = 356$ g/mol) (Fig. 4). The ^{13}C transverse relaxation times of **I** and **II** were determined by acquiring a series of ^{13}C spin-echoes with (T_2) and without (T_2^*) ^{1}H decoupling. The latter relaxation times incorporate the effects of proton spin-flips. Also measured were the ^{13}C T_1 relaxation times. The determined relaxation times were used to calculate the effective relaxation times of coherences during the long evolution intervals. When ^{1}H decoupling is used, this involves coherences $C_{1,xy}$ and

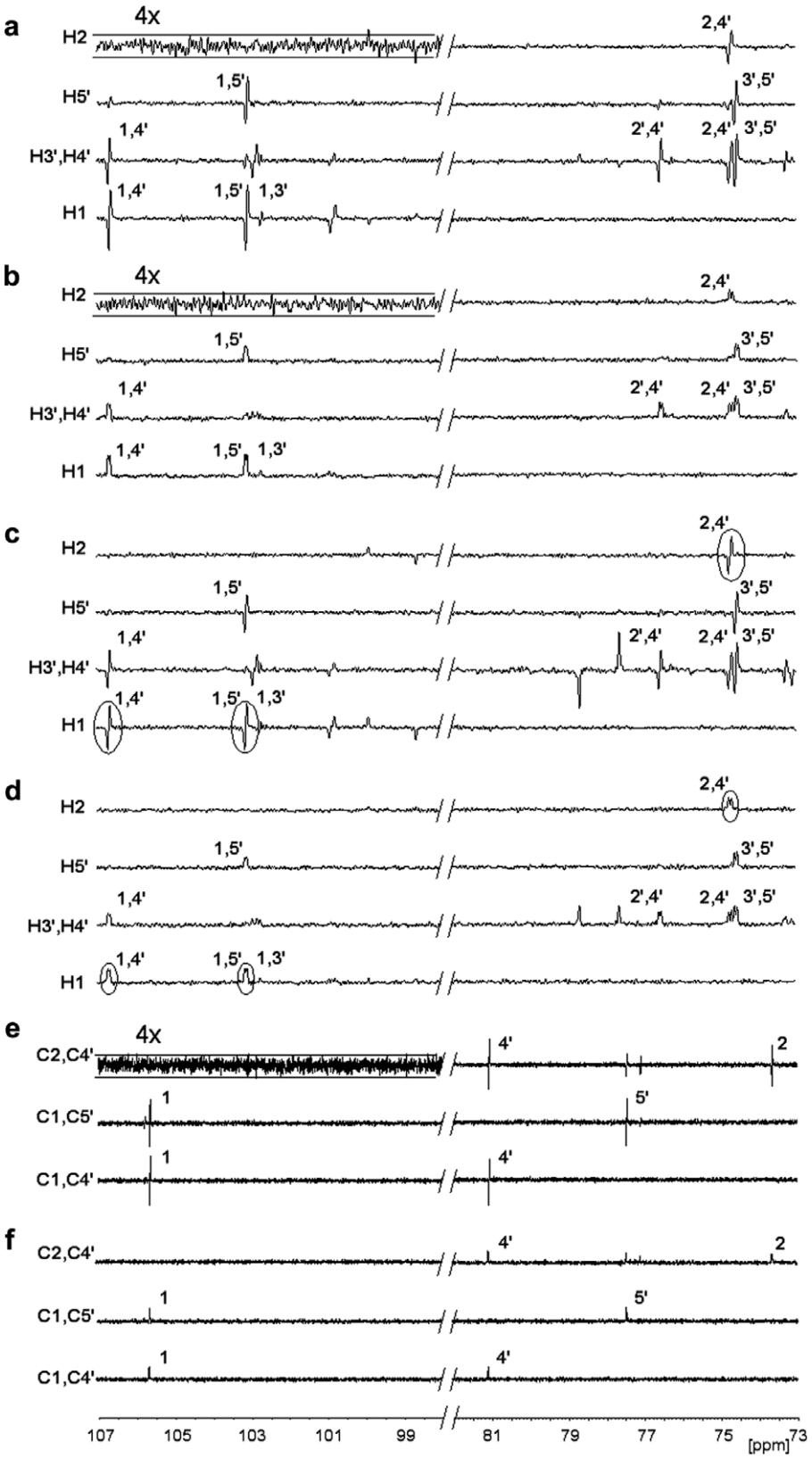

Fig. 2. Traces extracted from INADEQUATE spectra of **II**. (a–d) F_1 traces at F_2 ^{1}H chemical shifts of protons attached to carbons coupled to carbons of the other monosaccharide ring. (a) AP DEPT-INADEQUATE, (b) IP DEPT-INADEQUATE, (c) AP RINEPT-INADEQUATE, (d) IP RINEPT-INADEQUATE. The doublets circled in (c) and (d) are analyzed in Fig. 7. (e) and (f) Equivalent F_2 traces taken from ^{13}C-detected AP and IP INADEQUATE spectra of **II** [13]. All spectra were plotted using vertical scales yielding identical noise levels, as indicated in (a), (b) and (e) using empty regions of the spectra scaled up four times.

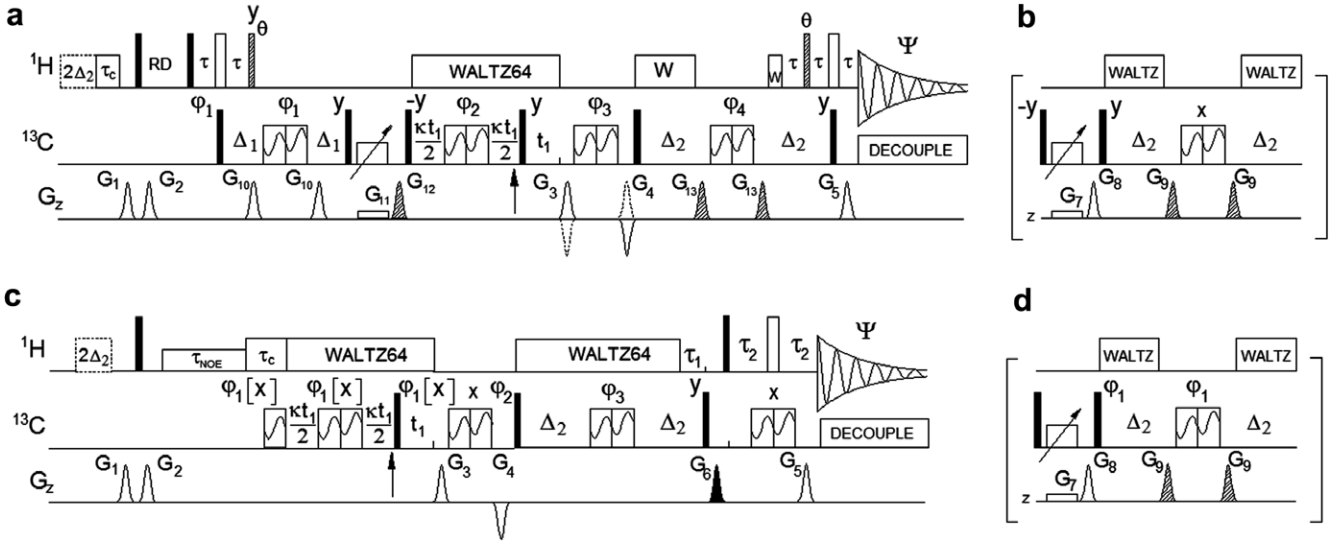

Fig. 3. Pulse sequences of ^{1}H-detected IPAP DEPT-INADEQUATE (a and b) and IPAP RINEPT-INADEQUATE experiments (c and d). Parts (b) and (d) are inserted at the position of the vertical arrows when in-phase doublets are acquired. The filled and open rectangles represent 90° and 180° rectangular pulses respectively, applied from the x axis unless stated otherwise. The dashed rectangles of the DEPT pulse sequence represent rectangular pulses with flip angle $\theta = 90°$ or 45°. The 90° BEBOP [40] and 180° BIBOP pulses [41] are indicated as wide rectangles with a sine wave. The ^{13}C adiabatic inversion pulses [37] are designated by an inclined arrow. The following delays were used: $\tau = 0.5/^{1}J_{CH}$, $\Delta_1 = 0.5/^{1}J_{CC}$, $\Delta_2 = 0.25/^{n}J_{CC}$, $\tau_1 = 0.5/^{1}J_{CH}$ for CH and $0.3/^{1}J_{CH}$ for all multiplicities, $\tau_2 = 0.25/1J_{CH}$. $T_{max} = \delta_{t1}(\kappa + 1)$*N, where δ_{t1}, κ, and N are the t_1 increment, J scaling factor and the number of increments per spectrum; $\tau_c = T_{max} - \delta_{t1}(\kappa + 1) * n$, where n is the actual t_1 increment number; $\tau_{NOE} = RD - T_{max} + \delta_{t1}(\kappa + 1) * n$, where RD is the relaxation delay. WALTZ decoupling during $2\Delta_2$, positioned at the beginning of the pulse sequences, indicted by dashed lines, is applied only when antiphase doublets are acquired. This, together with the WALTZ decoupling during the temperature compensating delay, τ_c, ensures that the temperature is constant over the entire duration of the experiment. The following phase cycling was applied in (a) and (b): $\varphi_1 = x, -x$; $\varphi_2 = 4x, 4(-x)$; $\varphi_3 = 2x, 2y$; $\varphi_4 = 8x, 8y$; $\Psi = 4(x,-x), 4(-x,x)$. PFGs expressed as a percentage of 50 Gcm^{-1} are: $G_1 = 60\%$, $G_2 = 70\%$, $G_3 = 40\%$, $G_4 = -40\%$, $G_5 = 40.16\%$, $G_7 = 4\%$, $G_8 = 15\%$, $G_9 = 90\%$, $G_{10} = 57\%$, $G_{11} = 4\%$, $G_{12} = 8\%$, $G_{13} = 77\%$. The following phase cycling was applied in (c) and (d): $\varphi_1 = x, y, -x, -y$; $\varphi_2 = 4x, 4(-x)$; $\varphi_3 = 8x, 8y$; $\Psi = 2(x,-x), 4(-x,x), 2(x,-x)$. For the acquisition of in-phase doublets the phase of the first three ^{13}C pulses is x as shown in square brackets and not φ_1. PFGs expressed as a percentage of 50 Gcm^{-1} are: $G_1 = 67\%$, $G_2 = 77\%$, $G_3 = 40\%$, $G_4 = -40\%$, $G_5 = 40.16\%$, $G_6 = 90\%$, $G_7 = 4\%$, $G_8 = 15\%$, $G_9 = 18\%$. All PFGs were shaped according to a CHIRP pulse [42], with an exception of long PFGs during adiabatic inversion, which were rectangular. The PFGs were applied during 1 ms, except for dashed and filled ones, which were 0.5 and 2 ms long, respectively. The echo-antiecho encoding of F_1 frequencies was achieved by changing the sign of G_3 and G_4 between successive t_1 increments.

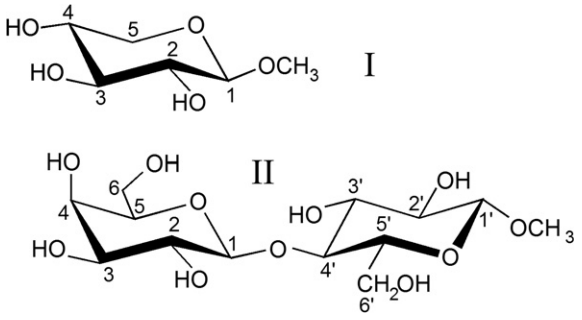

Fig. 4. Me-β-D−xylopyranoside, **I**, and Me-β-D-lactoside, **II**.

$C_{1,xy}$ $C_{2,z}$. As both exist for one half of a long-range evolution interval, their effective relaxation rate can be calculated [15] as:

$$[T_{2eff}(C_1)]^{-1} = [T_2(C_1)]^{-1} + 0.5 * [T_1(C_2)]^{-1}, \quad (1)$$

incorporating the effect of carbon spin-flips. The same equation can be used to calculate the T^*_{2eff} relaxation times in the presence of proton spin-flips by using T^*_2 instead of T_2. Fig. 5 shows a comparison of effective ^{13}C relaxation times, T_{2eff} and T^*_{2eff} calculated using Eq. (1) and T_2 or T^*_2 and T_1 values of the monosaccharide **I**, and disaccharide **II**. As expected, ^{1}H decoupling prolongs the lifetime of carbon coherences. The average values for the monosaccharide are $T_{2eff} = 1.70 * T^*_{2eff}$, while for the disaccharide $T_{2eff} = 1.45 * T^*_{2eff}$. A closer inspection of the data reveals that for carbons attached to protons with long T_1 relaxation times, such as H_2 of xylose or glucose, the gains of using the ^{1}H decoupling are modest. Also, the dipole–dipole transverse relaxation of carbons in CH_2 groups through two attached protons is the dominant relaxation mechanism leading to small increases of T_{2eff} over T^*_{2eff}. Nevertheless, for the majority of carbons the benefits of ^{1}H decoupling are significant.

Next, we compare the performance of several ^{1}H-detected INADEQUATE experiments (Fig. 1a) with and without [26] the ^{1}H decoupling. When the $H \rightarrow C \rightarrow H$ pathway is considered, either INEPT or DEPT can be used for polarization transfers. The latter requires fewer 180° ^{13}C pulses and was therefore applied. INEPT and DEPT have been used in the past in ^{13}C-detected INEPT- or DEPT-INADEQUATE experiments [30,31]. Fig. 1b shows a pulse sequence of ^{1}H-detected DEPT-INADEQUATE optimized for $^{n}J_{CC}$ coupling constants using DEPT for

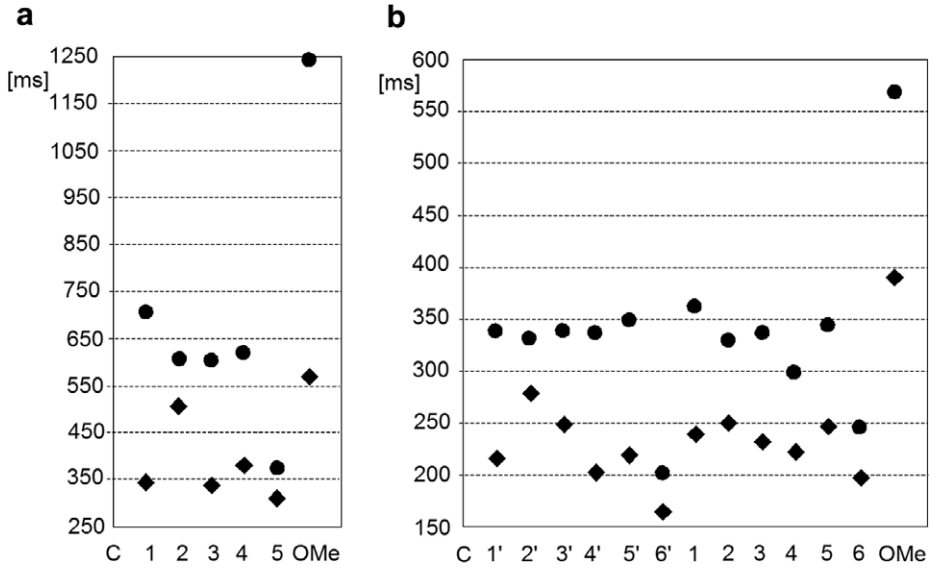

Fig. 5. Comparison of carbon spin–spin relaxation times in the presence ($T^{*}_{2\mathrm{eff}}$, ◆) and absence ($T_{2\mathrm{eff}}$, ●) of proton spin-flips. (a) and (b) show data for compounds **I** and **II** respectively.

both polarization transfer steps. A RINEPT-INADEQUATE, utilising the C → H pathway, is shown in Fig. 1c. The ^{1}H decoupling is used in both experiments during most of the J and DQ evolution intervals, except for short periods when the pulsed field gradients are applied. No measures were taken to eliminate the one-bond correlations in these experiments, which appear with random intensities. If required, their removal is possible as illustrated later. The pulse sequences of Fig. 1b and c can be fully optimized only for CH groups, while only a compromised setting is possible when all multiplicities are of interest. In the DEPT-INADEQUATE this choice is made by setting flip angles, θ, of two ^{1}H pulses, while in the RINEPT-INADEQUATE a single refocusing interval, τ_1, is set accordingly.

Fig. 6 contains F_2 traces extracted from 2D INADQUATE spectra of **I** acquired using various pulse sequences of Fig. 1 but otherwise identical experimental conditions. In the INEPT-INADEQUATE experiment (Fig. 1a) the refocusing of proton–carbon couplings is not used. This means that all carbon multiplicities will always have optimal sensitivity; however, this experiment is more susceptible to the relaxation effects. In addition, as pointed out by Sørensen et. al. [32], refocusing of carbon coherences with regard $^{1}J_{\mathrm{CH}}$ coupling constants prior to creating DQ coherences has an additional advantage when correlating protonated carbons. The losses through ZQ-coherences are minimised, increasing the signal by a factor of two. This gain is pertinent to both INADEQUATE experiments with ^{1}H decoupling (Fig. 1b and c), which in

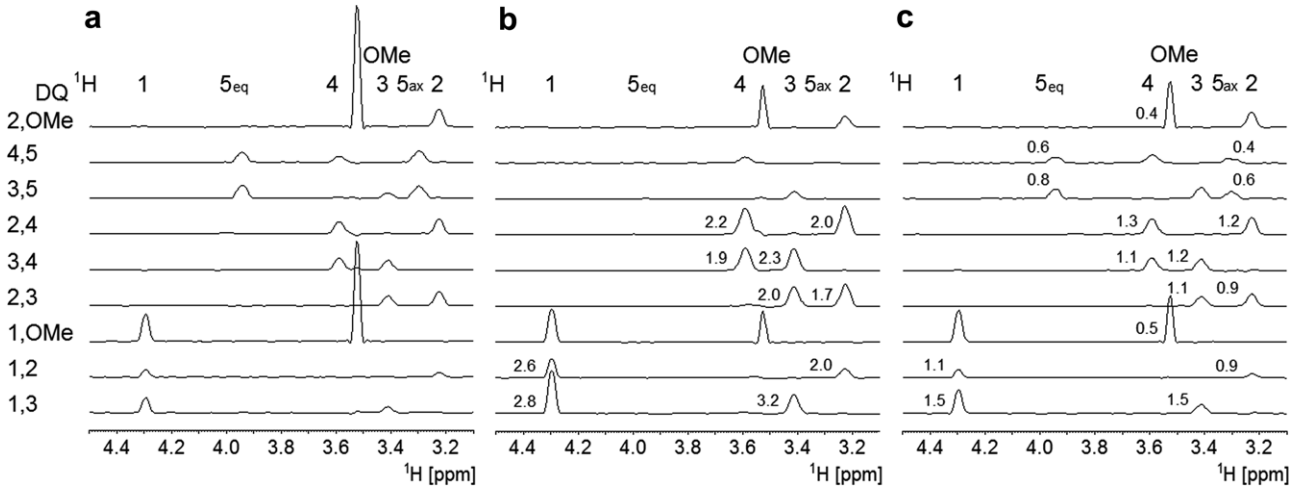

Fig. 6. F_2 traces showing carbon–carbon correlations of **I** extracted from ^{1}H-detected 2D INEPT-INADEQUATE (a), DEPT-INADEQUATE (b) and RINEPT-INADEQUATE (c). Intensities, relative to the corresponding cross peaks in (a), are shown in (b) and (c).

addition, are expected to be more resilient towards the relaxation effects. The DEPT-INADEQUATE experiment was optimised for CH groups ($\theta_1 = \theta_2 = 90°$), while the RINEPT-INADEQUATE experiment was optimized for all multiplicities ($\tau = 2.0$ ms). The rational behind these settings is as follows. The presence of two polarization transfer steps will significantly affect the intensity of all correlations when a compromise ($\theta_1 = \theta_2 = 45°$) setting is attempted in the DEPT-based experiment [30]. It is therefore of interest to probe its maximum sensitivity by focusing on CH carbons. On the other hand, the RINEPT-based pulse sequence with only one polarization transfer step is more general and will incur smaller losses while covering all carbon multiplicities.

The results are summarized in Table 1, where also the theoretical transfer efficiencies calculated by neglecting the relaxation effects are given. On average, larger than predicted gains were observed experimentally for CH–CH correlations in the DEPT-INADEQUATE spectra (2.27 vs 2.0). This result is clearly attributable to the relaxation effects, which for example are considerable for C_1C_3 correlations. The observed factors of 2.8 and 3.2 (see Fig. 6) can be rationalised by the fact that $T_{2\text{eff}} \sim 2^* T^*_{2\text{eff}}$ for C_1 and C_3 (see Fig. 5). The same cross peaks also show larger than average relative signal intensities (1.55 vs 1.18) in the RINEPT-INADEQUATE spectra.

Even though the sensitivity increases attributable to the relaxation effects are equal in the DEPT- and RINEPT-based experiments no extra gains were noticeable when comparing the theoretical (1.2) and average experimental (1.18) signal enhancements in the RINEPT-INADEQUATE spectrum. This indicates that some negative factors are acting in the latter experiments. All experiments were acquired using a uniform relaxation delay of 1.3 s, yet in **I**, the average T_1 relaxation time of ^{13}C-attached protons (0.8 s) is shorter than the average ^{13}C T_1 relaxation time (1.2 s). This decreases the relative sensitivity of the RINEPT-INADEQUATE compared to INEPT-INADEQUATE for this particular experimental setting. Fast repetition rates are also responsible for an incomplete build up of heteronuclear NOEs. These two factors also caused the experimental intensity of CH_3–CH correlations (0.42) to come close to the corresponding theoretical intensities (0.41). This is despite the fact that larger gains were expected based on $T_{2\text{eff}} \gg T^*_{2\text{eff}}$ for CH_3 groups (see Fig. 5). The theoretical relative intensities of CH_2 groups (0.71) in the RINEPT-INADEQUATE experiment are comparable to the average experimental ones (0.6).

Finally, a comparison of the experimental relative signal intensities of CH–CH correlation between the DEPT-INADEQUATE and RINEPT-INADEQUATE experiments (2.27:1.18) shows that the DEPT-based experiment is approximately twice as sensitive as the RINEPT-based experiment optimized for all multiplicities. However, when the DEPT-INADEQUATE was optimized for all multiplicities, as anticipated, the intensities of CH–CH correlations halved. The CH_2 groups reappeared, but their intensity was only 50% of those in the RINEPT-INADEQUATE spectra.

The above observations allow us to conclude this part of the work. When only CH–CH, CH–C, and CH–CH_2 correlations are of interest, the optimal experiment for tracing out the long-range carbon–carbon correlations is the DEPT-INADEQUATE incorporating ^{1}H decoupling during the long-range evolution intervals. When all carbon multiplicities are present, the original INEPT-INADEQUATE [26] followed by the RINEPT-INADEQUATE are overall more sensitive experiments. In the next, the experiments discussed above are converted into *J*-modulated experiments.

Table 1
Theoretical[a] and experimental cross peak intensities of **I** of three INADEQUATE experiments

Experiment/CH_x	CH	CH_2[h]	CH_3
INEPT-INADEQUATE	$4^{d} * 0.5^{e} = 2$ 1/*1*	$4^{d} * 0.5^{e} = 2$ 1/*1*	$4^{d} * 0.5^{e} = 2$ 1/*1*
DEPT-INADEQUATE[b]	4^{d} 2/*2.27*	[i]	[j]
RINEPT-INADEQUATE[c]	$3^{f} * 0.81^{g}$ 1.2/*1.18*	$3^{f} * 0.47^{g}$ 0.71/*0.6*	$3^{f} * 0.27^{g}$ 0.41/*0.42*

[a] Relaxation effects are not considered, *x*/*y* theoretical/*experimental* intensities normalized relative to the INEPT-INADEQUATE.
[b] Optimized for CH only.
[c] Optimized for all multiplicities.
[d] γ_H/γ_C.
[e] Intensity losses through ZQ-coherences [32].
[f] Heteronuclear NOE.
[g] Setting of the refocusing interval to 1/3.3*J*.
[h] CH_2–CH correlations only.
[i] Not observed.
[j] Not evaluated, appeared due to a mismatch between the actual and set $^1J_{CH}$ values.

3.2. J-modulated INADEQUATE experiments

The pulse sequence of ^{1}H-detected IPAP DEPT-INADEQUATE (Fig. 3a) was obtained by modifying the pulse sequence of the DEPT-INADEQUATE (Fig. 1b) using the principles outlined in [13,14,16]. Briefly, after transferring the proton magnetization to carbons, the one-bond ^{13}C–^{13}C couplings are allowed to evolve during $2\Delta_1 = 1/2^1J_{CC}$ only to be suppressed by a purging element that eliminates all but *z* magnetization [33]. This purging scheme does not require time averaging unlike a *z* filter implemented in MQ spectroscopy [34]. The evolution of long-range couplings during $2\Delta_1$ is marginal and the magnetization of long-range coupled carbons is therefore only slightly attenuated. Our experiments performed using ^{13}C-1 labeled glucose indicate that around 10% of the signal is lost because of the one-bond filter. The $2\Delta_1$ interval also serves to refocus the one-bond proton–carbon couplings. After the return of the carbon magnetization to the transverse plain, the following events take place: *J*-evolution, creation, frequency labelling and PFG encoding of

DQ coherences, back transfer of DQ to SQ ^{13}C coherences, their refocusing with respect to the long-range carbon–carbon couplings, short defocusing of one-bond proton–carbon couplings for reverse DEPT transfer, gradient decoding and finally, the detection of proton magnetization. Wherever possible, the ^{1}H decoupling is applied during the pulse sequence. This experiment produces antiphase doublets of long-range coupled carbons in F_1. As a consequence of κ-times faster incrementation of the J-evolution period relative to the DQ frequency labelling, F_1 doublets show an apparent splitting of κJ. For recording the in-phase doublets, a purging element that only selects the cosine modulated signal after the J-modulation period is inserted (Fig. 3b) followed by the defocusing of long-range carbon–carbon couplings.

The pulse sequence of the ^{1}H-detected IPAP RINEPT-INADEQAUATE (Fig. 3c and d) was obtained by modifying the pulse sequence of the RINEPT-INADEQUATE (Fig. 1c). Starting the polarization transfer pathway on ^{13}C makes this experiment simpler compared to the DEPT-based experiment. Following the build up of the heteronuclear NOEs during the relaxation delay, the pulse sequence starts with a J-modulation interval. From this point onwards the DEPT and RINEPT pulse sequences are identical with the exception of the final magnetization transfer to protons for which the DEPT and INEPT were used, respectively.

Fig. 2 shows selected F_1 traces extracted from a 2D IPAP DEPT-INADEQUATE and IPAP RINEPT-INADEQUATE spectra of **II** containing inter ring correlations. Both spectra were acquired using identical conditions and optimized for CH groups only. Their quality is comparable, with the DEPT-based experiments yielding higher signal-to-noise (S/N) ratios. Based on the analysis of the in-phase long-range cross peaks, factors of 1.1–1.7 (an average of 1.33) were observed. This is a smaller gain than that predicted by the theory (1.67:1). This observation can be explained by the fact that the DEPT-based experiment is more complicated and includes purging of one-bond correlations.

3.3. Extraction of coupling constants

It has been demonstrated that the editing of in-phase and antiphase multiplets provides accurate values of coupling constants only when the relationship between the intensities of the two multiplets is known [35]. In INADEQUATE experiments discussed here the intensity of the in-phase doublets is always lower, sometimes significantly. This is primarily because of the mismatch between the actual and set $^{n}J_{CC}$ coupling constant. In addition, extended evolution periods of the refocused experiments incur additional signal losses due to relaxation effects. It should be said that the accuracy of the scaling factors between the two types of doublets does not need to be high. Their overestimation leads to smaller errors than their underestimation. The reader is referred to the reference [13] for a detailed discussion. This finding is fortuitous, as low signal-to-noise ratio of INADEQUATE spectra will inevitably affect the accuracy of the determined scaling factors. These are, for the antiphase doublets, calculated as:

$$S_a = A(v)\sin(\pi J_{\mathrm{ini}} 2\Delta_2)\exp(-2\Delta_2/T_{2\mathrm{eff}}), \tag{2}$$

where J_{ini} is the initial coupling constants estimated as described below, $2\Delta_2$ is the length of the refocusing interval. $A(v)(\leqslant 1)$ is a factor that accounts for the fact that the refocused pulse sequence contains more pulses. The intensity of in-phase multiplets will therefore also be affected more by pulse imperfections and off resonance effects than that of the antiphase multiplets. This correction factor is, in principle, frequency dependent, and follows the excitation profile of the 90° rectangular pulse used to flip the magnetization into the z-axis prior to the purging of ZQ/DQ coherences. All other broad band pulses are offset independent. For a narrow spread of ^{13}C chemical shifts, such as carbohydrates used in this study, this frequency dependence can be safely ignored. A uniform correction factor, $A = 0.9$, as determined using a ^{13}C-1 labeled glucose sample, was employed in this work. When a short 90° broad-band universal rotator with negligible off resonance effects becomes available, it is advisable to use it instead of the remaining rectangular 90° pulses. This will remove the frequency dependence of A.

The initial coupling constant required for Eq. (1) is determined as follows. A resolved, long-range (or a one-bond) in-phase doublet is used as a reference peak, for which the carbon–carbon coupling constant is determined by peak picking. All in-phase long-range doublets are integrated either by using an integration routine or signal deconvolution. The ratio of the actual and the reference integral is used to determine the value of J_{ini} according to Eq. (3). This equation also takes into account the differences in effective relaxation times of different pairs of coupled carbons.

$$J_{\mathrm{ini}} = \frac{1}{2\pi\Delta_2}\arcsin\left(\left(\frac{I}{I_{\mathrm{ref}}}C(T_1)\right)^{1/2} \times \frac{\sin(\pi J_{\mathrm{ref}} 2\Delta_2)\exp\left(-2\Delta_2/T_{2\mathrm{eff}}^{\mathrm{ref}}\right)}{\exp(-2\Delta_2/T_{2\mathrm{eff}})}\right), \tag{3}$$

where I_{ref} and I are the integrals of the in-phase cross peaks of the reference and investigated doublet; J_{ref} and J_{ini} and $T_{2\mathrm{eff}}^{\mathrm{ref}}$ and $T_{2\mathrm{eff}}$ are the corresponding coupling constants and effective carbon spin–spin relaxation times. The latter are calculated using Eq. (1) and the measured spin–lattice and spin–spin ^{13}C relaxation times. In these relaxation experiments ^{1}H decoupling is applied during the inversion recovery and spin-echo delays, respectively. Given the concentrations required for INADEQAUTE experiments, such relaxation data are obtained in a matter of minutes. $C(T_1)$ is the correction factor that accounts for the variations in the T_1-driven signal recovery during the relaxation delay, RD:

$$C(T_1) = \frac{1 - \exp(-\mathrm{RD}/T_{1\mathrm{ref}})}{1 - \exp(-\mathrm{RD}/T_1)}, \quad (4)$$

where T_1 and $T_{1\mathrm{ref}}$ are the spin–lattice relaxation times of ^{13}C-attached protons (DEPT-INADEQUATE) or ^{13}C relaxation times (RINEPT-INADEQUATE). The ^{13}C relaxation times are also required for the determination of $T_{2\mathrm{eff}}$ and are easily obtained as explained above. The determination of T_1 relaxation times of ^{13}C-attached protons is more problematic, as it requires a selection of ^{13}C satellites in ^{1}H spectra. The overlap in ^{1}H spectra may prevent their accurate determination, but 1D inversion recovery concatenated with a 1D HSQC experiment will give reasonable estimates.

In order to facilitate the implementation of these experiments, we have investigated the effects of an imperfect recovery on signal intensities. For relaxation delays of $\geqslant 2T_{1\max}$ and a two fold difference between $T_{1\min}$ and $T_{1\max}$, the difference in the intensity of the recovered signal is 13%. This contributes marginally to the error of the scaling factor and can be safely ignored. We therefore recommend using relaxation delays twice as long as the longest T_1 relaxation times of spins used for the initial polarization transfer. In compound **II** the ^{1}H relaxation times ^{13}C-attached protons in CH groups ranged from 0.25 to 0.45 s, while the CH carbons had their T_1 relaxation times in the range of 0.4–0.6 s. The relaxation delays of 1 and 1.3 s were therefore used in the DEPT- and RINEPT-based experiments and $C(T_1)$ was set to 1.

When none of the long-range cross peaks are resolved, a one-bond cross peak could be used as reference signals. Unlike suggested previously [13], there is no additional contribution to the effective carbon spin–spin relaxation times caused by the ^{13}C–^{13}C dipolar relaxation of directly bonded carbon pairs. To support this statement, T_1 and T_2 relaxation times of C-2 in α and β anomers were measured in both unlabeled and ^{13}C-1 labeled glucose. The T_1 relaxation times were identical for both samples. $T_{2\mathrm{eff}}$ of ^{13}C-1 labeled glucose were calculated using Eq. (1). These agreed well with the measured values, thus fully explaining faster relaxation of the labelled samples by considering the contribution of the ^{13}C-1 carbon spin-flips. This makes the one-bond cross peaks an attractive alternative to the long-range cross peaks to act as reference signals and can be used to analyze the coupling constants in the IPAP RINEPT-INADEQUATE spectra.

In summary, the scaling factor for the antiphase doublets required for spectral editing is determined using Eqs. (1)–(4). In these calculation $C(T_1) = 1$ and $A(v) = 0.9$ can be used when the conditions explained above have been satisfied. This exercise requires the measurement of carbon T_1 and T_2 relaxation times.

Fig. 7 contains an example of the coupling constant analysis showing the extraction of one large (3.1 Hz) and two small (both 2.0 Hz) interglycosidic coupling constants of **II**. Despite using $\kappa = 4$ to acquire the spectra, the latter two doublets are at the border line of possible extraction of coupling constants from in-phase multiplets only. All long-range coupling constants extracted from both DEPT- and INEPT-based experiments are given in Table 2. Please note a good agreement between the values obtained in the two experiments.

4. Discussion

Here we compare the theoretical and experimental sensitivities of the new ^{1}H-detected INADEQUATE experiments with those of the related ^{13}C detected INADEQUATE experiment [13]. The theoretical gains of the ^{1}H-detected version can be calculated [36] as $0.71^*(\gamma_H/\gamma_C)^{5/2}/3 = 7.6$, where factors 0.71 and 3 account for the use of PFGs in the ^{1}H-detected experiments and the utilization of the heteronuclear NOE in the ^{13}C-detected experiment, respectively. As noted by others [37], such large sensitivity gains are rarely achieved. This is mainly because of a combination of ^{1}H-^{1}H couplings and short

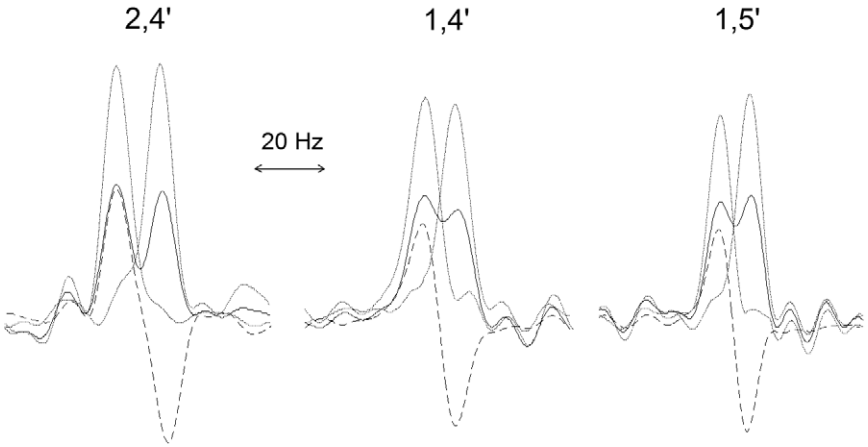

Fig. 7. Analysis of interglycosidic coupling constants of **II** using traces from IPAP RINEPT-INADEQUATE spectra (circled doublets in Fig. 2c and d). The scaling factors used for antiphase doublets (dashed lines), obtained as explained in the text, were 0.46, 0.52 and 0.52 from left to right. The dotted lines are the sum or the difference of the in-phase and antiphase doublets.

Table 2
Long-range ^{13}C–^{13}C coupling constants, in Hz, of **II**[a]

Experiment/carbon pair	13	24	35	16	1′3′	2′4′	3′5′
DEPT-INADEQUATE	4.9/[b]	[c]	1.7/1.5	4.3/[f]	4.4/[b]	2.5/2.4	2.5[e]
INEPT-INADEQUATE	[b]	[c]	[d]/1.4	4.1/[f]	4.6/[b]	2.4/2.4	2.5[e]
Experiment/carbon pair	1′6′	13′	14′	15′	24′	1′OMe	2′OMe
DEPT-INADEQUATE	3.7/[f]	0.6/[b]	1.9/2.0	2.0/2.0	3.1/3.1	2.1/2.0	3.4/3.1
INEPT-INADEQUATE	3.9/[f]	0.5/[b]	[d]/2.0	2.1/2.1	3.1/3.1	2.1/[f]	3.1/[f]

[a] Determined from two cross peaks in each spectrum whenever possible.
[b] Low S/N ratio.
[c] No coupling [43].
[d] Overlap.
[e] Reference coupling.
[f] Cross peak not present.

acquisition times leading to large line widths (tens of Hz) of the acquired signals in ^{1}H-detected INADEQUATE, which compares unfavorably with ^{13}C detection where the lines are only few Hz wide. The lack of proton–carbon polarization transfer steps in ^{13}C-detected INADEQUATE and the simplicity of this experiment increase its sensitivity.

Experimental comparison of both approaches is illustrated in Fig. 2, where also the traces extracted from 2D ^{13}C detected IPAP INADEQUATE spectra [13] of **II** are presented using C_1,$C_{4'}$, C_1,$C_{5'}$, C_2,$C_{4'}$ correlations. Although the t_1 (^{1}H detection) and t_2 (^{13}C detection) noise have different character (see expansions in Fig. 2a, b and e), all spectra were plotted in such a way as to present the same noise levels. Please note that the effective coupling evolution cannot be scaled up in the F_2 dimension of the ^{13}C-detected IPAP INADEQUATE, while a factor of $\kappa = 4$ was used in the ^{1}H-detected experiments. This explains the different appearance of cross peaks between the two types of spectra.

The average S/N for 1D traces of the inter ring cross peaks shown in Fig. 2 was 1.4 (IP) and 1.1 (AP) times higher in the IPAP DEPT-INADEQUATE spectra than in the ^{13}C-detected IPAP INADEQUATE spectra. When IP cross peaks were integrated in both spectra, those in the ^{1}H-detected spectrum were on average two times more intense. This is a consequence of a larger frequency space (κJ) covered by these cross peaks in F_1 in the ^{1}H-detected spectra. Such cross peaks are less affected by random noise fluctuations and provide coupling constants with higher precession. Although all experiments were acquired using identical spectrometer time and optimized for the same $^{n}J_{CC} = 3.0$ Hz, ^{1}H-detected experiments were acquired on a 600 MHz cryoprobe instrument (S/N of EtBz $\sim$ 4500:1), while the ^{13}C-detected experiments were obtained using an 800 MHz cryoprobe with a cold carbon preamplifier (^{13}C S/N of EtBz $\sim$ 1000:1). Had the ^{1}H-detected experiments been acquired on the 800 MHz instrument (S/N of EtBz $\sim$ 9000:1), their performance would have improved approximately two times. On the other hand, if a 500–600 MHz ^{13}C dedicated cryoprobe (^{13}C S/N of EtBz $\sim$ 1800:1) was used, the S/N of the ^{13}C-detected experiment would also improve approximately two times. It should be noted that to date most of the cryoprobes have inner ^{1}H coils. In conclusion, the arguments presented above give good reasons as to why ^{1}H-detected INADEQUATE experiments have their place in the repertoire of NMR experiments for the measurement of $^{n}J_{CC}$ coupling constants, despite the fact tat they fall short of sensitivity gains indicated by a simple comparison of proton and carbon gyromagnetic ratios.

The $^{3}J_{CC}$ coupling constants are extremely valuable for the conformational analysis of carbohydrates as they complement $^{n}J_{CH}$ coupling constants [38], which by themselves do not fully characterise the conformation of the flexible glycosidic linkage of the carbohydrate molecules [39]. Coupling constants $^{3}J_{C1,C5'} = 2.0$ Hz $^{3}J_{C2,C4'} = 3.1$ Hz were obtained for **II**. Very weak cross peaks were observed for the third pair of inter glycosidic carbons, C1, C3′. Their analysis yielded a coupling constant of $\sim$0.5 Hz. These coupling constants, obtained previously using selectively ^{13}C-enriched carbohydrates, enabled characterization of the glycosidic dihedral angles of **II** [39].

The S/N ratios obtained in 42 h for in-phase and antiphase multiplets in the ^{1}H-detected IPAP DEPT-INADEQUATE spectra of the disaccharide **II** were 9–21:1, or 13.5:1 in average. This indicates that 25 mg of a larger molecule, e.g. a tetrasaccharide, would still yield, after the addition/subtraction of the in-phase and antiphase doublets, S/N ratios close to 10:1 on a 600 MHz cryoprobe, which is sufficient for accurate coupling constant determination.

5. Conclusions

We have proposed new ^{1}H-detected INADEQUATE experiments optimized for long-range ^{13}C–^{13}C correlation. Refocusing of $^{1}J_{CH}$ coupling constants and the use of ^{1}H-decoupling in these experiments significantly enhanced their performance when compared to the ^{1}H-detected INADEQUATE methods currently used to establish one-bond correlations. Full benefits of this approach are realized by the DEPT-INADEQUATE experiment optimized for CH–CH, CH–C and CH–CH_2 correlations. The acquisition of in-phase and antiphase doublets in F_1 is proposed for the measurement of $^{n}J_{CC}$ coupling constants in ^{1}H-detected IPAP DEPT-INADEQUATE and IPAP RIN-

EPT-INADEQUATE experiments. Editing of in-phase and antiphase doublets is shown to yield accurate values of long-range carbon–carbon coupling constants from poorly resolved doublets. These techniques can be used to measure small interglycosidic coupling constants of carbohydrates using ~100 mM samples. A comparison with an analogous ^{13}C-detected IPAP INADEQUATE experiment shows that ^{1}H-detected IPAP DEPT-INADEQUATE optimized for CH correlations yields on today's cryoprobes at least two times better S/N than afforded by ^{13}C-detection on ^{1}H-dedicated cryoprobes with a cold ^{13}C preamplifier. A setting for all multiplicities leads to a similar performance of both methods.

Acknowledgments

L.J. acknowledges the support of the ORS scheme, K.E.K. thanks the financial support from the Hungarian Scientific Research Fund OTKA T 048713 and NK 68578.

References

[1] M.L. Severson, G.E. Maciel, A molecular–orbital study of the dihedral angle dependencies of vicinal carbon–carbon coupling-constants, J. Magn. Reson. 57 (1984) 248–268.
[2] D.L. Krivdin, E.W. Della, Spin–spin coupling constants between carbons separated by more than one bond, Prog. Nucl. Magn. Reson. 23 (1991) 301–610.
[3] M. Eberstadt, G. Gemmecker, D.F. Mierke, H. Kessler, Scalar coupling constants—their analysis and their application for the elucidation of structures, Angew. Chem. Int. Ed. 34 (1995) 1671–1695.
[4] T.J. Church, I. Carmichael, A.S. Serianni, Two-bond ^{13}C–^{13}C spin-coupling constants in carbohydrates: effect of structure on coupling magnitude and sign, Carbohydr. Res. 280 (1996) 177–186.
[5] B. Bose, S. Zhao, R. Stenutz, F. Cloran, P.B. Bondo, G. Bondo, B. Hertz, I. Carmichael, A.S. Serianni, Three-bond C–O–C–C spin-coupling constants in carbohydrates: development of a Karplus relationship, J. Am. Chem. Soc. 120 (1998) 11158–11173.
[6] L.B. Krivdin, Non-empirical calculations of NMR indirect carbon–carbon coupling constants. Part 4: bicycloalkanes, Magn. Reson. Chem. 41 (2003) 417–430.
[7] A. Bax, R. Freeman, S.P. Kempsell, Natural abundance ^{13}C–^{13}C coupling observed via double-quantum coherence, J. Am. Chem. Soc. 102 (1980) 4849–4851.
[8] A. Bax, R. Freeman, T.A. Frenkiel, M.H. Levitt, Assignment of ^{13}C NMR-spectra via double-quantum coherence, J. Magn. Reson. 43 (1981) 478–483.
[9] A. Bax, R. Freeman, S.P. Kempsell, Investigation of ^{13}C–^{13}C long-range couplings in natural-abundance samples, J. Magn. Reson. 41 (1980) 349–353.
[10] N.C. Nielsen, H. Bildsøe, H.J. Jakobsen, O.W. Sørensen, Editing of ^{13}C–^{13}C satellite spectra, J. Magn. Reson. 78 (1988) 223–244.
[11] L. Ma, P. Bigler, Simultaneous measurement of one-bond and long-range carbon–carbon coupling-constants in cembrene, Magn. Reson. Chem. 30 (1992) 1247–1254.
[12] T. Fäcke, S. Berger, Application of a gradient-enhanced measurement for carbon–carbon coupling-constants (GRECCO) to a conformational study of geraniol and (*E*,*E*)-farnesol, J. Am. Chem. Soc. 117 (1995) 9547–9550.
[13] L. Jin, D. Uhrín, ^{13}C-detected IPAP-INADEQUATE for simultaneous measurement of one-bond and long-range scalar or residual dipolar coupling constants, Magn. Reson. Chem. 45 (2007) 628–633.
[14] W. Kozminski, D. Nanz, Sensitive measurement and unambiguous assignment of long-range ^{13}C–^{13}C coupling constants at natural isotope abundance, J. Magn. Reson. Ser. A 122 (1996) 245–247.
[15] B. Reif, M. Köck, R. Kerssebaum, J. Schleucher, C. Griesinger, Determination of ^{1}J, ^{2}J, and ^{3}J carbon–carbon coupling constants at natural abundance, J. Magn. Reson. Ser. B 112 (1996) 295–301.
[16] K.E. Kövér, P. Forgó, J-modulated ADEQUATE (JM-ADEQUATE) experiment for accurate measurement of carbon–carbon coupling constants, J. Magn. Reson. 166 (2004) 47–52.
[17] T.N. Pham, K.E. Kövér, L. Jin, D. Uhrín, ^{1}H-Detected Double-J-Modulated INEPT-INADEQUATE for simultaneous determination of one-bond and long-range carbon–carbon connectivities and the measurement of all carbon–carbon coupling constants, J. Magn. Reson. 176 (2005) 199–206.
[18] W. Kozminski, D. Sperandio, D. Nanz, Sensitive measurement of one-bond carbon–carbon spin coupling constants at natural isotope abundance, Magn. Reson. Chem. 34 (1996) 311–315.
[19] A. Bax, L. Lerner, Measurement of ^{1}H–^{1}H coupling-constants in DNA fragments by 2D NMR, J. Magn. Reson. 70 (1988) 429–438.
[20] D. Uhrín, T. Liptaj, Determination and assignment of heteronuclear long-range coupling-constants—methods based on semiselective INEPT, J. Magn. Reson. 81 (1989) 82–91.
[21] H. Kessler, A. Müller, H. Oschkinat, Differences and sums of traces within COSY spectra (DISCO) for the extraction of coupling-constants—decoupling after the measurement, Magn. Reson. Chem. 23 (1985) 844–852.
[22] J. Keeler, D. Neuhaus, J.J. Titman, A convenient technique for the measurement and assignment of long-range ^{13}C proton coupling-constants, Chem. Phys. Lett. 146 (1988) 545–548.
[23] D. Uhrín, V. Varma, J.R. Brisson, A method for measurement of long-range heteronuclear coupling constants from 2D HMQC spectra, J. Magn. Reson. Ser. A 119 (1996) 120–124.
[24] R.A.E. Edden, J. Keeler, Development of a method for the measurement of long-range ^{13}C–^{1}H coupling constants from HMBC spectra, J. Magn. Reson. 166 (2004) 53–68.
[25] M. Ottiger, F. Delaglio, A. Bax, Measurement of J and dipolar couplings from simplified two-dimensional NMR spectra, J. Magn. Reson. 131 (1998) 373–378.
[26] J. Weigelt, G. Otting, ^{1}H-detected INEPT-INADEQUATE at natural ^{13}C abundance, J. Magn. Reson. Ser. A 113 (1995) 128–130.
[27] A. Bax, M. Ikura, L.E. Kay, D.A. Torchia, R. Tschudin, Comparison of different modes of two-dimensional reverse-correlation NMR for the study of proteins, J. Magn. Reson. 86 (1990) 304–318.
[28] D. Uhrín, S. Uhrínova, C. Leadbeater, J. Nairn, N.C. Price, P.N. Barlow, 3D $HCCH_3$-TOCSY for resonance assignment of methyl-containing side chains in ^{13}C labeled proteins, J. Magn. Reson. 142 (2000) 288–293.
[29] P.J. Keller, K.E. Vogele, Sensitivity enhancement of INADEQUATE by proton monitoring, J. Magn. Reson. 68 (1986) 389–392.
[30] O.W. Sørensen, R. Freeman, T. Frenkiel, T.H. Mareci, R. Schuck, Observation of C-13–C-13 couplings with enhanced sensitivity, J. Magn. Reson. 46 (1982) 180–184.
[31] S.W. Sparks, P.D. Ellis, DEPT polarization transfer for the INADEQUATE experiments, J. Magn. Reson. 62 (1985) 1–11.
[32] A. Meissner, D. Moskau, N.C. Nielsen, O.W. Sørensen, Proton-detected ^{13}C–^{13}C double quantum coherence, J. Magn. Reson. 124 (1997) 245–249.
[33] J. Thrippleton, J. Keeler, Elimination of zero-quantum interference in two-dimensional NMR spectra, Angew. Chem. Int. Ed. Engl. 42 (2003) 3938–3941.
[34] M. Rance, O.W. Sørensen, W. Leupin, H. Kogler, K. Wütrich, R.R. Ernst, Uniform excitation of multiple-quantum coherence. Application to two-dimensional double-quantum spectroscopy, J. Magn. Reson. 61 (1985) 67–80.
[35] F. Delaglio, Z.R. Wu, A. Bax, Measurement of homonuclear proton couplings from regular 2D COSY spectra, J. Magn. Reson. 149 (2001) 276–281.

[36] F.J.M van de Ven, Multidimensional NMR in liquids, in: Basic Principles and Experimental Methods, Wiley-VCH, New York.
[37] J. Buddrus, J. Lambert, Connectivities in molecules by INADEQUATE: recent developments, Magn. Reson. Chem. 40 (2002) 3–23.
[38] I. Tvaroška, M. Hricovíni, E. Petráková, An attempt to derive a new Karplus-type equation of vicinal proton carbon coupling-constants for C–O–C–H segments of bonded atoms, Carbohydr. Res. 189 (1989) 359–362.
[39] B. Bose, S. Zhao, R. Stenutz, F. Cloran, P.B. Bonodo, G. Bondo, B. Hertz, I. Carmichael, A.S. Serianni, Three-bond C–O–C–C spin-coupling constants in carbohydrates: Development of a Karplus relationship, J. Am. Chem. Soc. 120 (1998) 11158–11173.
[40] T.E. Skinner, T.O. Reiss, B. Luy, N. Khaneja, S.J. Glaser, Reducing the duration of broadband excitation pulses using optimal control with limited RF amplitude, J. Magn. Reson. 167 (2004) 68–74.
[41] B. Luy, K. Kobzar, T.E. Skinner, N. Khaneja, S.J. Glaser, Construction of universal rotations from point-to-point transformations, J. Magn. Reson. 176 (2005) 179–186.
[42] J.M. Bohlen, I. Burghardt, M. Rey, G. Bodenhausen, Frequency-modulated CHIRP pulses for broad-band inversion recovery in magnetic-resonance, J. Magn. Reson. 90 (1990) 183–191.
[43] C. Thibaudeau, R. Stenutz, B. Hertz, T. Klepach, S. Zhao, Q. Wu, I. Carmichael, A.S. Serianni, Correlated C–C and C–O bond conformations in saccharide hydroxymethyl groups: parametrization and application of redundant ^{1}H–^{1}H, ^{13}C–^{1}H, and ^{13}C–^{13}C NMR J-couplings, J. Am. Chem. Soc. 126 (2004) 15669–15685.